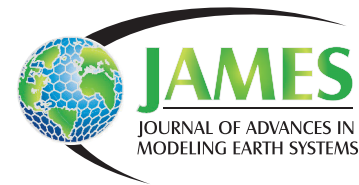


Tropical Cyclone Activity Downscaled from NOAA-CIRES Reanalysis, 1908-1958



Kerry Emanuel

Program in Atmospheres, Oceans, and Climate, Massachusetts Institute of Technology, Cambridge, Massachusetts

Manuscript submitted 31 October 2009; in final form 5 January 2010

A recently developed technique for deducing tropical cyclone activity from global reanalyses and climate models is applied to a reanalysis of the global atmosphere during the period 1908-1958. This reanalysis assimilates only sea surface temperature, sea ice, and surface pressure observations, which are relatively homogeneous over the period. The downscaling technique has been shown to produce results in good agreement with observations of tropical cyclones when driven by reanalyses over the period 1980-2006, a period when global tropical cyclone frequency was robustly observed.

When applied to the 1908-1958 reanalysis, the derived global frequency of tropical cyclones shows no significant trend over the period, while the frequency of events in the southern hemisphere shows a statistically significant decline and that of the northern hemisphere shows a marginally significant increase. There are statistically significant increases in frequency over the period in the North Atlantic, eastern North Pacific, and northern Indian Oceans, while frequency declines in the western North Pacific. Power dissipation estimates from best-track data are highly correlated with the power dissipation of downscaled events in the Atlantic, though the amplitude of the variability and trends of the downscaled power dissipation are smaller than those of the best-track estimates by about a factor of two.

A recently developed genesis index applied to the reanalysis data is highly correlated with downscaled event frequency on regional spatial scales, but is largely uncorrelated at the scale of the globe and even on the scale of large tropical cyclone-producing regions such as the western North Pacific.

Finally, while it is tempting to believe that specification of sea surface temperature is sufficient for capturing most aspects of the general state of the atmosphere relevant to tropical cyclones, we show, using simple arguments, that failure to account for changing radiative properties of the atmosphere can distort the response of tropical cyclone activity to changing distributions of sea surface temperature; moreover, models appear to systematically underestimate the response of near-tropopause temperatures to changing surface temperature, and this too can affect the response of potential intensity.

DOI:10.3894/JAMES.2010.2.1

1. Introduction

The effect of climate change on tropical cyclone activity is a matter of great practical concern and inherent intellectual interest. One approach to quantifying the relationship between tropical cyclones and climate is to relate historically observed metrics of storm activity to metrics of climate (such as ENSO or sea surface temperature). While relatively straightforward, historical data sets are short, particularly outside the North Atlantic region, and suffer numerous quality issues, as documented for example by Landsea et al. (2004) and Emanuel (2005). Another approach is to detect tropical cyclones in simulations of the global climate and attempt to relate their statistics to various aspects of the

simulated climate. This approach has been taken by numerous groups (e.g. Bengtsson et al., 1996, Sugi et al., 2002, Oouchi et al., 2006, Yoshimura et al., 2006, Bengtsson et al., 2007) and is becoming more popular as the horizontal resolution of global climate models improves. But even horizontal grid spacing as low as 20 km (Oouchi et al., 2006) cannot resolve the critical eyewall region of the cyclones, and invariably the maximum wind speed of simulated storms is truncated at relatively low values by the lack of horizontal resolution (Zhao et al., 2009). Recent work by Rotunno et al. (2009) suggests that horizontal grid spacing of less than 1 km is needed to properly resolve intense storms. Furthermore, global climate models con-

To whom correspondence should be addressed.

Kerry Emanuel, Rm. 54-1620, MIT, 77 Massachusetts Avenue, Cambridge, MA 02139, USA
emanuel@mit.edu



This work is licensed under a Creative Commons Attribution 3.0 License.

tinue to show wide divergence in the regional responses of tropical cyclone activity to climate change (e.g. Emanuel et al., 2008), at least in part because of the wide regional divergence of such elementary quantities as surface enthalpy fluxes and precipitation among the various models.

Another approach to quantifying the relationship between climate and tropical cyclone activity is to “down-scale” tropical cyclone activity from reanalysis data sets, as pioneered by Knutson et al. (2007) and Emanuel et al. (2008). Such techniques involve running high-resolution, detailed models capable of resolving tropical cyclones, using boundary conditions supplied by the reanalysis data sets. This combines the advantage of relatively robust estimates of large-scale conditions by the reanalysis with the high fidelity simulation of tropical cyclones by the embedded high-resolution models. As shown by Knutson et al. (2007) and Emanuel et al. (2008), these techniques are remarkably successful in reproducing observed tropical cyclone climatology in the period 1980-2006, particularly in the North Atlantic region, when driven by NCAR-NCEP reanalysis data (Kalnay and co-authors, 1996). In spite of the success of these downscaling methods, problems arise in attempting to drive them with reanalysis data from before roughly 1980. The philosophy employed in creating the two most frequently used reanalysis data sets (NCAR/NCEP and ERA40) is to assimilate into them all available observations that meet quality control standards. Unfortunately, the type and number of such observations evolves through time, introducing systematic biases into the reanalyses. This is particularly a problem around 1979, when satellite-based radiance observations began to be assimilated, causing a discontinuity in time series of such quantities as high troposphere temperature (Santer and co-authors, 1999). This influences downscaled tropical cyclone activity by, for example, causing a bias in the estimated potential intensity (Bister and Emanuel, 2002).

Most recently, there have been attempts to reanalyze the global atmosphere using only observed sea surface temperature, sea ice, and surface pressure observations (Compo et al., 2006, 2008), relying on the model to reproduce the three-dimensional structure of the time-evolving state. While such efforts suffer from a relative lack of observational constraints above the surface, they have the advantage that the number and type of observations of pressure, sea ice, and sea surface temperature are relative homogeneous through the period, so that the time series of the atmospheric state may be relatively free of strong biases.

An early attempt at such a reduced reanalysis has recently been undertaken (Compo et al., 2006, 2008)¹, spanning the period 1908-1958. We apply the tropical cyclone downscaling method of Emanuel et al. (2008) to estimate tropical cyclone activity globally during this period². Briefly, this

¹ The reanalysis data are available at http://www.cdc.noaa.gov/data/gridded/data.20thC_Rean.html.

² We do not here simulate tropical cyclones in the South Atlantic.

method embeds a specialized, atmosphere-ocean coupled tropical cyclone intensity model in the large-scale atmosphere-ocean environment represented by the global reanalysis data. The tropical cyclone model is initialized from weak, warm-core vortices seeded randomly in space and time, and whose movement is determined with a beta-and-advection model driven by the flows derived from the reanalysis wind fields. The thermodynamic state used by the intensity model is also derived from the reanalysis data together with climatological estimates of ocean mixed layer depths and sub-mixed layer thermal stratification, and the wind shear input to the intensity model is likewise derived from the reanalysis wind fields. In practice, a large proportion of the initial seeds fail to amplify to at least tropical storm strength and are discarded; the survivors are regarded as constituting an estimate of the tropical cyclone climatology for the given climate state. (Details of the technique are described in Emanuel et al., 2008.) For the present purpose, we run 200 events in each of five sections of the world oceans in each of the 51 years spanning 1908-1958. For the Atlantic, this represents an ensemble of roughly 20 members, given that there are roughly 10 events per year in that basin. The frequency of events is derived from the ratio of the number of storms (200 in this case) to the number of seeds planted, multiplied by a single, model-dependent rate constant.

Section 2 describes the results of this exercise, and section 3 presents some important caveats in interpreting climate trends in models driven solely by changing surface conditions (such as sea surface temperature) but without changing the radiative properties of the atmosphere. Results are summarized in section 4.

2. Results

2.1. Global and regional variability

Figure 1 shows the annual frequency of global events together with the northern and southern hemispheres individually. Here the rate constant has been chosen to yield 90 global events annually, averaged over the 51 year period. The global frequency over the period is virtually constant (there is an insignificant downward trend with a p value of 0.19), but there is a significant ($p \approx 0$) negative trend in the southern hemisphere, with the annual frequency declining from about 40 in 1908 to around 33 in 1958. The northern hemisphere shows a marginally insignificant ($p \approx 0.06$) upward trend.

The annual frequencies in specific regions of the northern hemisphere are shown together with corresponding linear trends in Figure 2. The trends in all cases are statistically significant at least the 5% level; the trend is negative in the western North Pacific and positive elsewhere.

The frequencies appear to be anomalously low in the eastern North Pacific; this is confirmed by comparing the annual mean frequencies in each basin, averaged over the 51 years, to observed frequencies in the interval 1980-2006

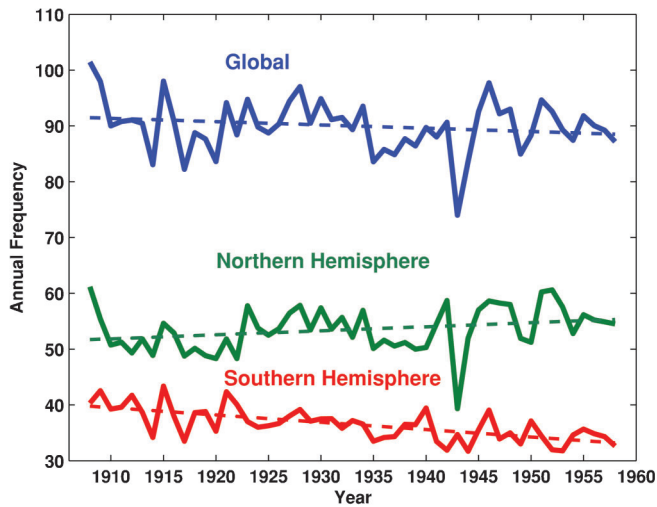


Figure 1: Annual tropical cyclone frequency from downscaling the NOAA-CIRES 20th century reanalysis from 1908 to 1958, together with linear trends over the period. Top curve: global total; middle curve: Northern Hemisphere; bottom curve: Southern Hemisphere.

(well within the satellite era), as shown in Figure 3. Under-representation of the eastern North Pacific was also noted in the downscaling of the NCAR/NCEP reanalysis during the period 1980–2006 (Emanuel et al., 2008). Elsewhere, it is not clear how much of the differences are artifacts of the technique and how much may be real differences between the earlier and later periods.

While the frequency of tropical cyclones is of some inherent interest, as a practical matter, most damage and loss of life results from the highest intensity events (Pielke and Landsea, 1998). A better metric of the destructive potential of a tropical cyclone is the power dissipation index

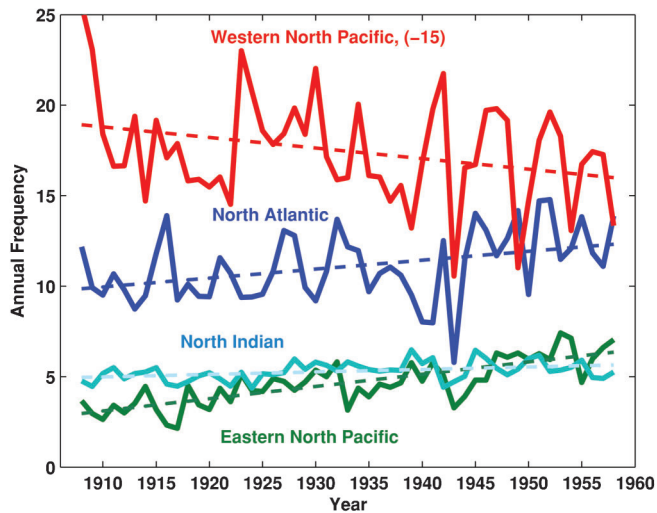


Figure 2: Annual number of tropical cyclones in regions of the Northern Hemisphere, with linear trends shown. Note that 15 storms have been subtracted from the western North Pacific totals for comparison purposes.

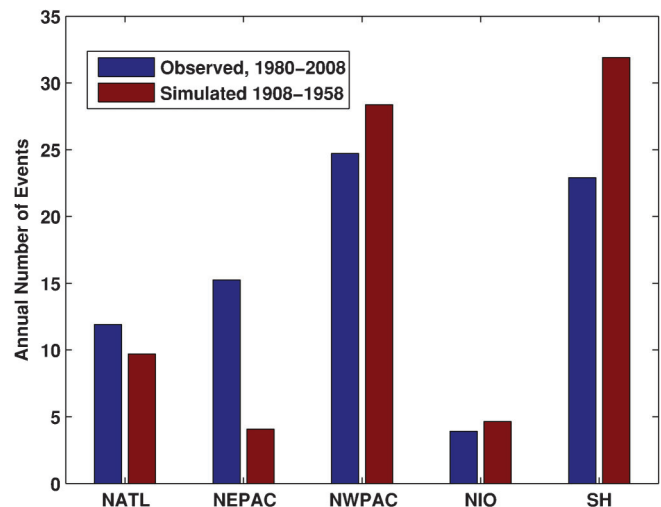


Figure 3: Mean annual downscaled storm counts for each basin over the period 1908–1958 (red bars) compared to observed annual mean counts or the period 1980–2008 (blue bars).

(Emanuel, 2005), which is defined as the integral over the lifetime of the event of its maximum surface wind speed cubed. If it were possible to integrate this quantity over the surface area covered by the storm, this would measure the total kinetic energy dissipated by the storm over its lifetime (Emanuel, 2005). Sriver and Huber (2006) showed, however, that the power dissipation index is an adequate measure of the total power dissipation.

Figure 4 shows the annual power dissipation of the downscaled storms over the globe, and for each hemisphere. There is a small but statistically significant increase in power dissipation in the Northern Hemisphere, and a larger and significant decrease in the southern hemisphere, yielding a small but still significant decrease in power dissipation over the globe.

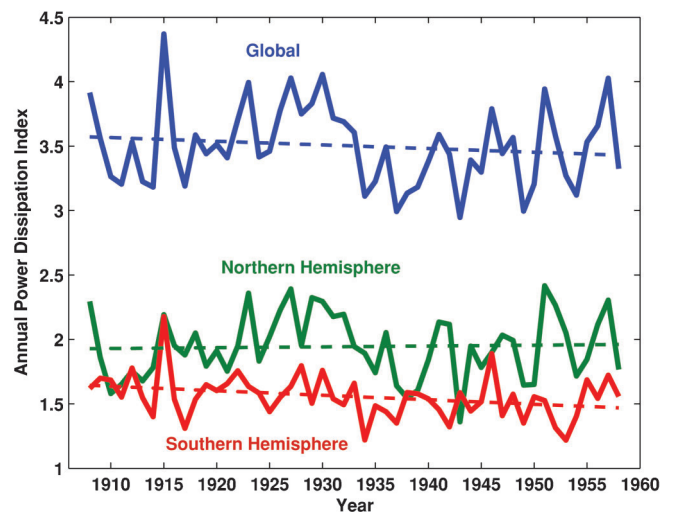


Figure 4: Downscaled annual tropical cyclone power dissipation and linear trends in each hemisphere and for the globe.

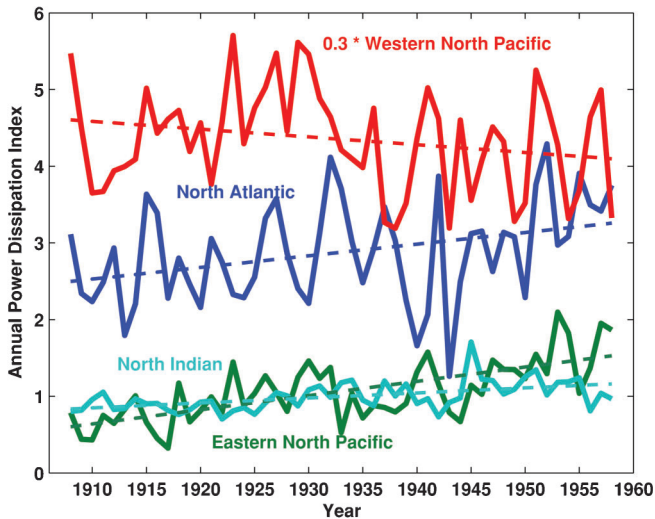


Figure 5: Downscaled tropical cyclone power dissipation and linear trends for tropical cyclone regions of the Northern Hemisphere. Note that western North Pacific values have been scaled by 0.3.

Power dissipation in individual basins in the northern hemisphere (Figure 5) follows the same general trends as event frequency, with a downward trend in the western North Pacific and upward trends elsewhere, all of them statistically significant at the 1% level. In the eastern Pacific, power dissipation increases by more than a factor of two over the period.

2.2. Comparison with best-track data for the North Atlantic

Evaluation of the quality of downscaled tropical cyclone metrics can only be conducted over the North Atlantic during the period 1908-1958. Elsewhere, during this pre-

satellite era, observations are too few and erratic to produce reliable estimates of tropical cyclone frequencies or other metrics (Emanuel, 2005). Figure 6a compares the annual frequency of events in the best-track data set (Neumann et al., 1999) to that of the downscaled events in the North Atlantic region. The two frequency time series are weakly correlated ($r^2=0.15$) and show statistically significant upward trends over the period, though the observed trend is more than twice the simulated trend.

Part of the reason for the larger trend in the best-track data may be that the frequency of storms might have been underestimated earlier in the record, prior to the advent of aircraft reconnaissance (Chang and Guo, 2007, Vecchi and Knutson, 2008). Figure 6b shows the result of applying the corrections to the best-track tropical storm record suggested by Vecchi and Knutson (2008). This clearly brings the two series into better alignment, but the linear trend of the corrected best-track data is still larger than that of the downscaled storms by a factor of 1.8. It is not clear whether this is because the degree to which the earlier storms had been undercounted was itself underestimated, because of difficulties in the downscaling, or because of random variability in the observed storms. It is noteworthy that the linear trend of the residual time series, i.e. the difference between the downscaled and corrected best-track frequencies, is not statistically significant ($p=0.28$). Since the downscaled events represent an effective ensemble size of about 20, one would expect the random component of the variance to be reduced by about a factor of 20 compared to the single realization of the historical events. Thus if the corrected best-track data and the downscaled events were drawn from the same population, the detrended residual time series should represent mostly random variability. The variance of the detrended residual time series is 11.6, compared to the time mean corrected best-track rate of

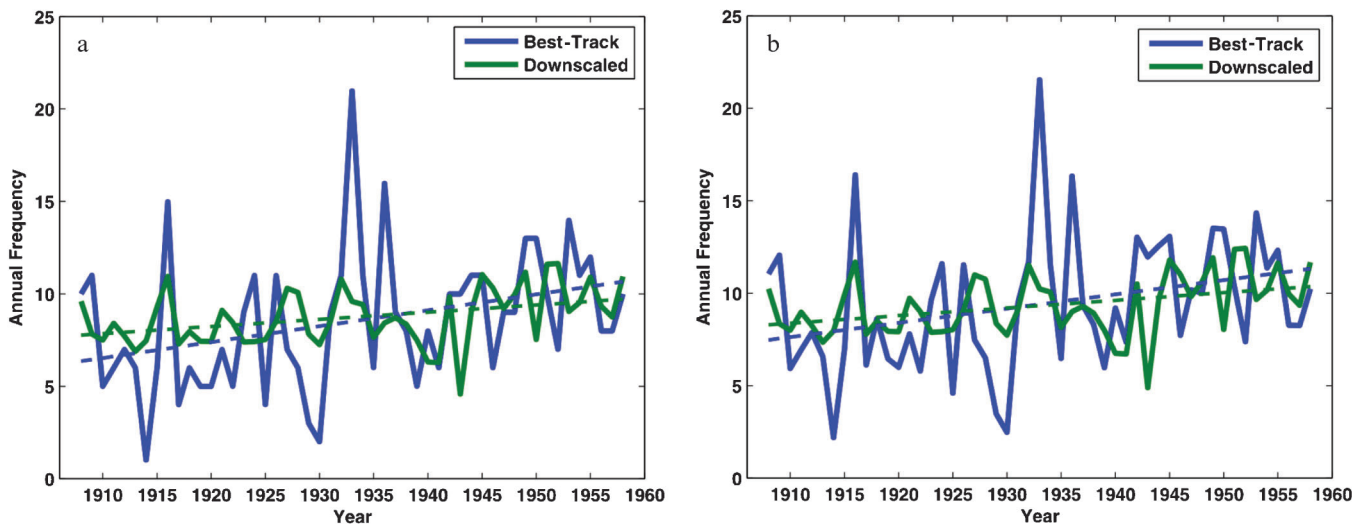


Figure 6: Downscaled annual tropical cyclone counts in the Atlantic (green curves) and linear trends compared to uncorrected best-track data (a) and best-track data corrected according to Vecchi and Knutson (2008) (b).

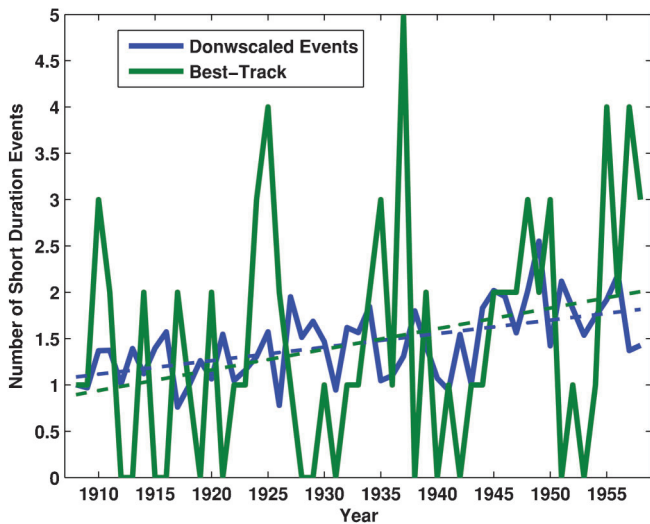


Figure 7: Annual number of downscaled short-duration events (blue) compared to best-track events (green), with linear trends superimposed.

9.4. If the residual time series represented a Poisson process, then its variance would equal its mean. The slightly higher residual variance than would be predicted in a Poisson process may indicate either that there is still some residual climate signal in the residual series, that the random component of variability does not have the character of a Poisson process, or that the corrected best-track data and the downscaled events are not after all drawn from the same population.

Figure 7 shows the times series of downscaled and best-track short-duration events (defined as events whose maximum duration of tropical-storm force winds is less than 48 hours), with linear trends superimposed. The number of downscaled short duration events increases from about 1.08

at the beginning of the 50-year period to about 1.82 events at the end, an increase of about 67%. Although there is a slightly greater increase in best-track events, the difference between the two trends is not significant ($p=0.55$). Thus it is not implausible that at least part of the upward trend in short duration events discussed by Landsea et al (2009) is real and not merely an artifact of improved observing capabilities. There is also a statistically significant upward trend of long-duration (> 48 hour) events over the period. This is consistent with Landsea et al (2009) when the same period of time is considered (see their figure 5).

Figure 8a shows times series of power dissipation from the (uncorrected) best-track data and from the downscaled events, with linear trends superimposed. There are highly significant positive trends in both estimates. At first glance, it would appear that the best-track-based power dissipation may suffer from the same underestimation problems that affect the storm counts, but there are two considerations that weigh against this interpretation. First, because power dissipation is heavily weighted toward strong and long-lasting events, it is unlikely that its annual total is much affected by the weak, short-lived systems that disproportionately explain the undercounts (Landsea et al., 2009). Second, it is apparent from Figure 8a that not only do the downscaled events underestimate the trend over the period, but they clearly underestimate, as well, the strong multi-year perturbations in the series, though the phasing of these perturbations is about right. Figure 8b presents the best linear fit of the downscaled power dissipation to the best-track series. The two series turn out to be very well correlated, ($r^2=0.64$), and the linear fit corrects all of the trend and much of the amplitude of the multi-year perturbations at the same time. The regression amplifies the trend and perturbations of the downscaled events by very nearly a factor of two.

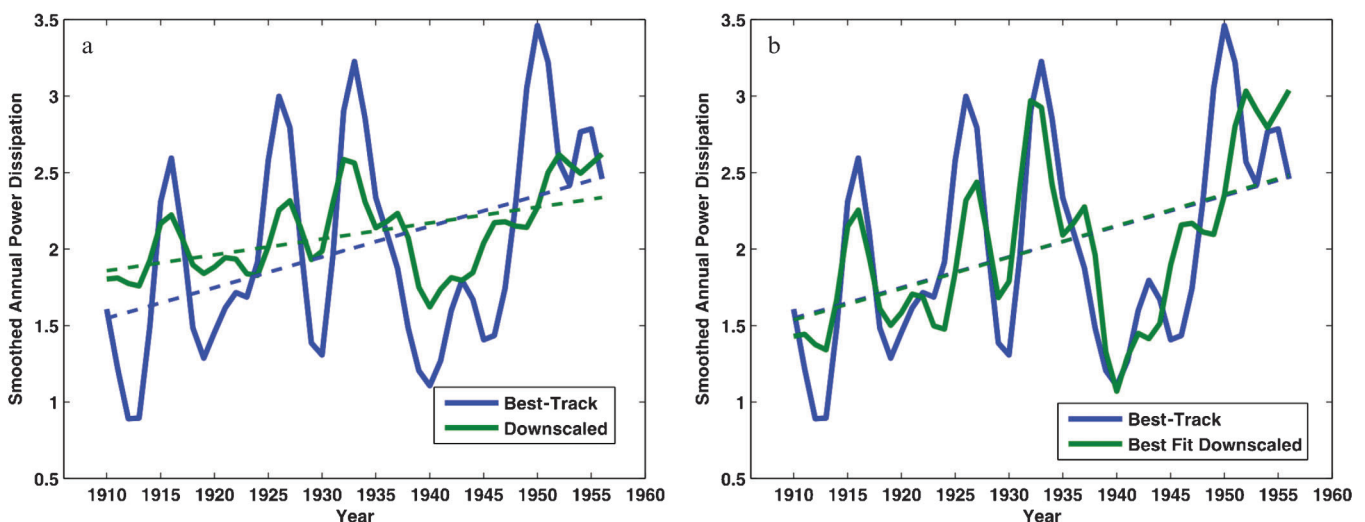


Figure 8: Annual Atlantic tropical cyclone power dissipation from downscaled events (green) and best-track events (blue), each smoothed with a 1-3-4-3-1 filter and with linear trends superimposed (a). In (b), the green curve denotes the best linear fit of the downscaled power dissipation to the power dissipation of the best-track data, each filtered with a 1-3-4-3-1 filter.

Clearly the downscaled power dissipation is less sensitive to climate perturbations than is the power dissipation of real world storms, by about a factor of two. In the next section, we shall argue that this is in part owing to the failure of the reanalysis to account for time-varying radiative properties of the atmosphere (which likely caused at least part of the observed variations of sea surface temperature) and in part because of potential problems in simulating the temperature of the very high troposphere.

2.3. Relationship of downscaled storm frequency to a genesis potential index

Over the past few decades there have been several attempts to empirically relate tropical cyclogenesis to large-scale environmental parameters thought to play a role in the formation of storms. These attempts date back to the work of Gray (1979), who used sea surface temperature, mid-level relative humidity, a measure of vertical wind shear, and low-level vorticity as predictors. More recently, Emanuel and Nolan (2004) developed an index based on potential intensity rather than sea surface temperature, and with other predictors similar to those used by Gray. Theoretical and modeling considerations suggest, however, that the dependence on water vapor should not be on relative humidity but on saturation deficit (Emanuel et al., 2008). This led us to develop a new formulation of the genesis potential index:

$$GPI \equiv |\eta|^3 \chi^{-4/3} \text{MAX}((V_{pot} - 35 \text{ ms}^{-1}), 0)^2 \times (25 \text{ ms}^{-1} + V_{shear})^{-4}, \quad (1)$$

where η is the absolute vorticity of the 850 hPa flow, V_{pot} is the potential intensity (Bister and Emanuel, 1998), V_{shear} is the magnitude of the 850 hPa-250 hPa wind shear, and

$$\chi \equiv \frac{s_b - s_m}{s_0^* - s_b},$$

where s_b , s_m , and s_0^* are the moist entropies of the boundary layer and middle troposphere, and the saturation moist entropy of the sea surface, respectively. The nondimensional parameter χ is thus a measure of the moist entropy deficit of the middle troposphere, which becomes larger as the middle troposphere becomes drier. Note that, unlike previous indices, (1) is (by design) dimensionally correct, yielding a rate per unit area per unit time. In developing (1), the fit to the annual cycle in each hemisphere and to the spatial distribution of observed genesis events has been optimized using monthly mean values of the environmental variables.

Figure 9 compares the globally integrated GPI with the global downscaled storm count. Here the GPI has also been normalized to give a global mean value of 90 over the period. Even though both time series have been smoothed in time, there is no significant correlation between the two series ($r^2=0.06$, $p=0.09$), and the GPI has a significant upward trend over the period, compared to the slight but insignificant downward trend of the downscaled events. Examination

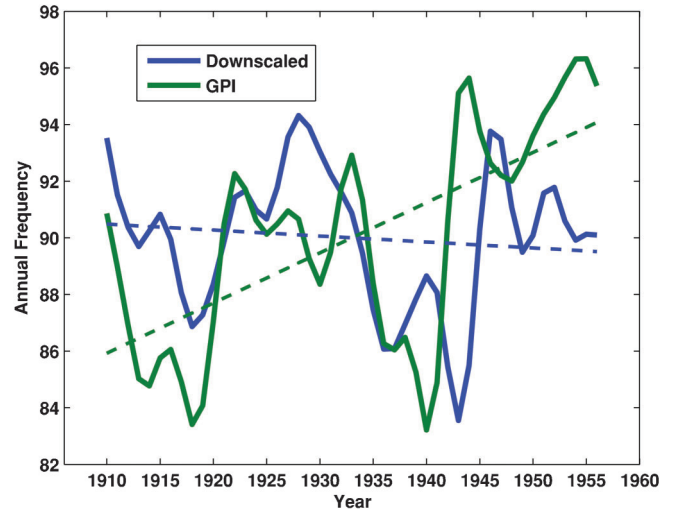


Figure 9: Globally integrated genesis potential index as given by (1) compared to annual global frequency of downscaled events (blue).

of the various factors in (1) reveals that it is primarily the decline of χ that is responsible for the increase in GPI over the period. The detrended time series are a little better correlated ($r^2=0.18$), but there is still not much skill in predicting global mean downscaled storm counts with the GPI .

The downscaled frequencies of events in each hemisphere are compared to the GPI s summed individually over each hemisphere in Figure 10. The GPI trend in positively biased in both hemispheres, but this time there is a highly significant correlation ($r^2=0.55$) between the smoothed GPI and the smoothed, downscaled frequencies in the northern hemisphere, and two series are also significantly correlated in the southern hemisphere ($r^2=0.13$, $p=0.01$). The GPI overestimates activity in the northern hemisphere and underestimates it in the southern hemisphere.

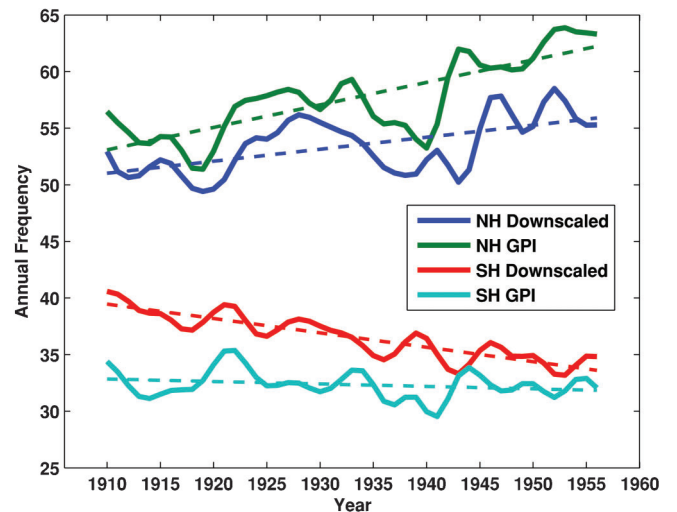


Figure 10: Comparison between annual frequencies in each hemisphere and hemispherically integrated GPI as given by (1).

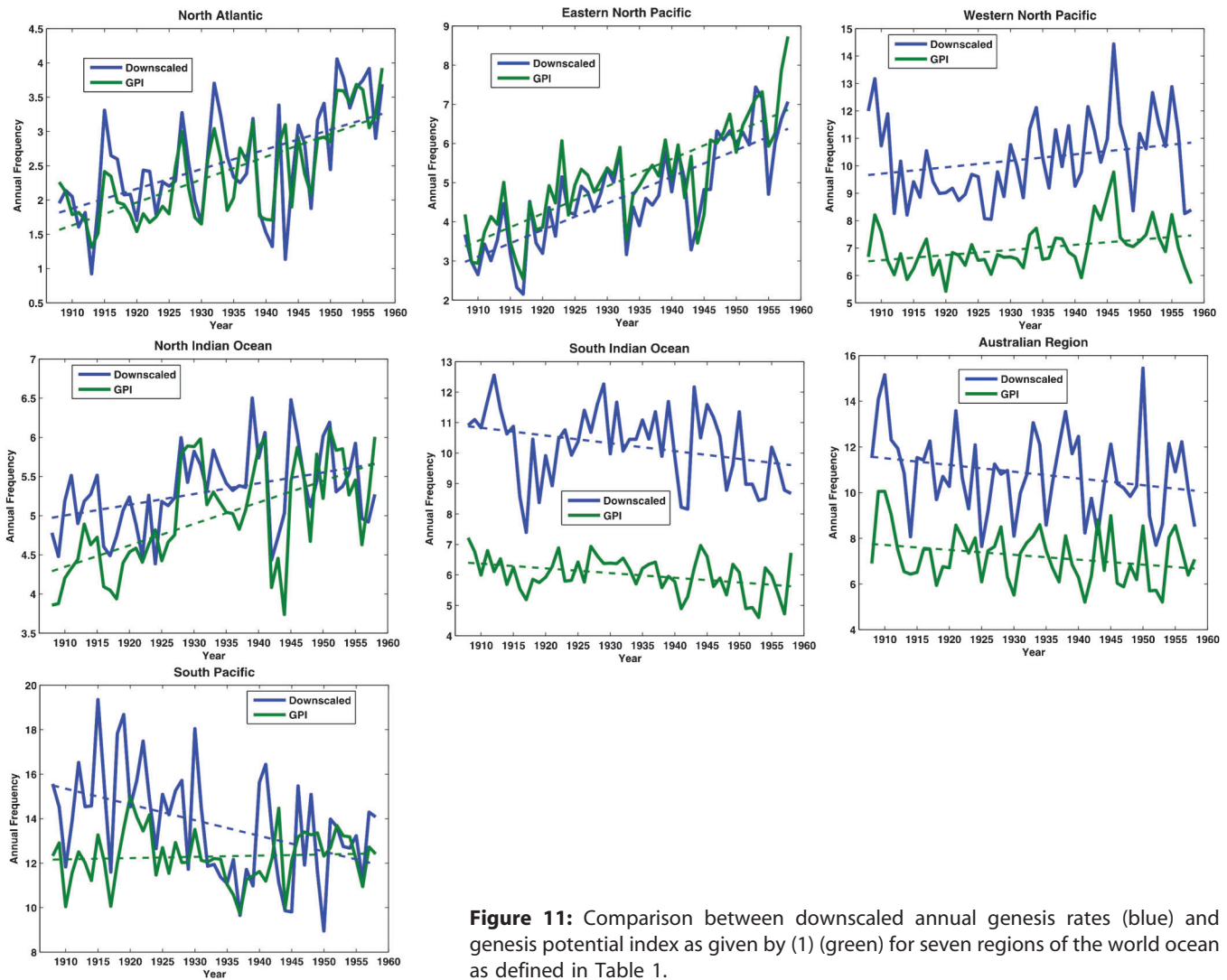


Figure 11: Comparison between downscaled annual genesis rates (blue) and genesis potential index as given by (1) (green) for seven regions of the world ocean as defined in Table 1.

As one goes down in scale to the regional level, the correlations between downscaled storm counts and the *GPI* improve. Figure 11 shows the time series of (unsmoothed) *GPI* and downscaled storm counts, each normalized to yield a global annual average of 90 events over the period, for seven regions of the world oceans defined in Table 1. In each case, the *GPI* and downscaled frequencies are highly significantly correlated, though the trends do not agree well in the South Pacific.

3. Caveats

3.1. Limitations of using AGCMs to downscale tropical cyclone activity

It is tempting to believe that specification of sea surface temperatures and other boundary conditions such as sea ice in a high quality model leads to an accurate estimate of the state of the atmosphere. The success of AGCMs such as the NOAA-CIRES 20th Century reanalysis in replicating key

features of the atmospheric circulations reinforces this idea. Specification of the sea surface temperature circumvents the need for surface energy balance, as would be the case in a coupled system in which the sea surface temperature is predicted. In general, there is no need for energy balance at the top of the atmosphere (TOA), since the ocean can act as a net heat source or sink when sea surface temperature is specified. Here we show that failure to achieve TOA energy balance will generally lead to an incorrect estimate of

Table 1: Definitions of Regions used in Figure 11

Region	Latitudes	Longitudes
North Atlantic	6-18 N	20-60 W
Eastern North Pacific	5-16 N	90-170 W
Western North Pacific	5-20 N	110-150 E
North Indian	5-20 N	50-110 E
South Indian	5-20 S	50-100 E
Australian	5-20 S	100-160 E
South Pacific	5-20 S	160 E-130 W

potential intensity even when the sea surface temperature is correct.

We begin with the conservation equation for the moist static energy, h :

$$\frac{\partial \rho h}{\partial t} + \nabla \bullet \rho \mathbf{V} h = - \frac{\partial}{\partial z} [F_{rad} + F_c], \quad (2)$$

where \mathbf{V} is the large-scale velocity, ρ is the air density, and F_{rad} and F_c are the energy fluxes by radiation and by small scale turbulence (including dry and moist convection). Integrating (2) through the depth of the atmosphere and assuming equilibrium (steady-state) conditions, we obtain

$$F_{c0} = F_{rad\ TOA} - F_{rad0} + \int_0^\infty [\nabla_2 \bullet \rho \mathbf{V} h] dz, \quad (3)$$

where F_{c0} is the surface turbulent net enthalpy flux, $F_{rad\ TOA}$ is the net top-of-the-atmosphere radiative flux, F_{rad0} is the net surface radiative flux, and the last term is the integral over the atmosphere of the horizontal divergence of the moist static energy flux by large-scale motions. The first two terms on the right side of (3) also represent the vertically integrated radiative cooling of the atmosphere.

Now if the ocean mixed layer is itself in thermodynamic equilibrium, then $F_{c0} + F_{rad0} = 0$, i.e. there is no net energy flux through the sea surface. In that case, according to (3), the TOA radiative flux balances the net convergence of energy into the column. If, however, the sea surface temperature is specified, there is no requirement for energy balance because the sea may act as a net source or sink of energy. Symbolically, we can write

$$F_{c0} = -F_{rad0} + E, \quad (4)$$

where E is the net energy source supplied by the ocean.

The turbulent flux of enthalpy at the sea surface may be represented by a bulk aerodynamic formula:

$$F_{c0} = C_k \rho_{10} |\mathbf{V}_{10}| (k_0^* - k_{10}), \quad (5)$$

where C_k is the enthalpy exchange coefficient appropriate to 10 m altitude, k_0^* is the saturation enthalpy of the sea surface, k_{10} is the enthalpy at 10 m, and elsewhere the subscript 10 denotes evaluation at 10 m. Combining (5) and (4) yields

$$k_0^* - k_{10} = \frac{-F_{rad0} + E}{C_k \rho_{10} |\mathbf{V}_{10}|}. \quad (6)$$

The left side of (6) represents the thermodynamic disequilibrium between the ocean and the atmosphere, the principle factor in the definition of potential intensity (Emanuel, 1986). Thus, if one holds the surface wind speed $|\mathbf{V}_{10}|$ fixed in (6), the potential intensity will vary with the net radiative flux into the ocean and the residual energy imbalance at the sea surface. In general, raising the sea surface temperature from its equilibrium value will increase both E

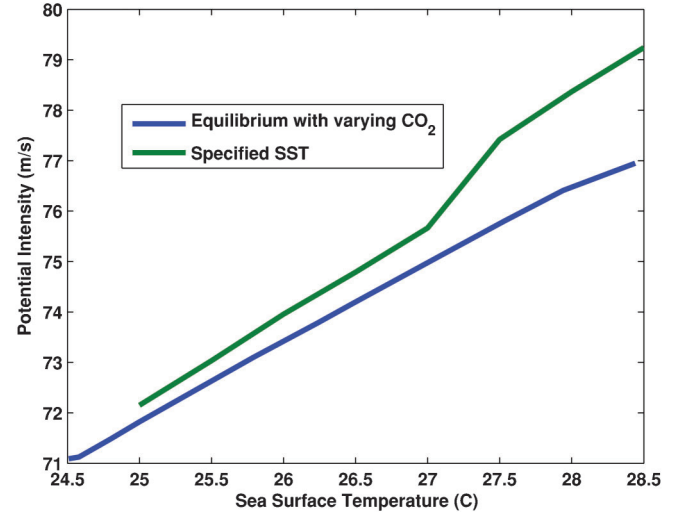


Figure 12: Variation of potential intensity with sea surface temperature in a single-column model run into a state of radiative convective equilibrium. Blue curve: specified sea surface temperature; Green curve: surface energy balance enforced with SST variation brought about by varying atmospheric CO₂.

and the net radiative flux into the sea, the latter arising from increasing atmospheric temperature and water vapor (assuming that clouds remain fixed). But, in general, this increase in back radiation is not enough to offset the imbalance term E in (4) or (6), thus both the convective flux and the sea surface thermodynamic disequilibrium increase faster for a specified increase in sea surface temperature than for an equilibrium increase (for which $E=0$) brought about by, say, an increase in carbon dioxide content.

This point is illustrated in Figure 12, which shows the potential intensity as a function of sea surface temperature produced by a radiative-convective equilibrium model (Rennó et al., 1994) run to equilibrium for specified sea surface temperature and for equilibrium sea surface temperature calculated using a slab ocean and varied by varying the concentration of CO₂ in the atmosphere. In these simulations, the distribution of clouds is held fixed but water vapor is permitted to vary according to the model's own hydrological cycle. In the calculation of potential intensity, the thermodynamic efficiency is held fixed so as to focus on the changes owing strictly to changes in the surface thermodynamic disequilibrium. When the sea surface temperature is specified, the rate of increase of potential intensity is about a third larger than when the sea surface temperature is in equilibrium with a specified CO₂ concentration.

Thus a fundamental limitation of using AGCMs to deduce tropical cyclone activity is that errors in the surface energy balance will lead to errors in potential intensity, which has a strong effect on both the intensity and frequency of tropical cyclones. For example, AGCMs run with specified increases of SST without a concomitant increase in surface radiative forcing may overpredict the increase in

potential intensity and thereby overpredict the response of tropical cyclone activity to warming. Thus the underprediction of the response of tropical cyclones to changing climate, so evident in Figure 8, is probably not related to the lack of surface energy balance in AGCMs.

3.2. Other considerations

It is evident from (6) that the sensitivity of air-sea thermodynamic disequilibrium to changing radiative forcing is highly sensitive to surface wind speed as it is represented in surface flux formulations. This is worrisome, as it is common, for example, to add “gustiness factors” to the calculation of mean wind in models, and this varies from model to model (Fairall et al., 2003). (This problem applies equally to coupled models and to AGCMs.) This may help explain why the tropical mean potential intensity varies by more than 30% among the seven 20th century climate simulations used in the downscaling study by Emanuel et al. (2008). This problem is compounded by differences in simulated mean surface winds among the various models, which is particularly acute in regions of low mean surface wind speeds, as is evident from (6).

Another problem arises from the difficulty that GCMs experience in simulating trends in temperature in the upper troposphere and lower stratosphere (Cordero and Forster, 2006). This affects the potential intensity by influencing the altitude, and therefore the temperature, at which air flowing up through the eyewall of a hurricane attains neutral buoyancy with respect to its environment; this is known as the “outflow temperature” (Emanuel, 1986). For the downscaling simulations described here, the outflow temperature is calculated in the course of finding the potential intensity using the algorithm discussed in Bister and Emanuel (2002). While the outflow temperature is often confused with the temperature at a fixed altitude, it is also a function of the entropy of parcels ascending in the eyewall, and therefore of the sea surface temperature.

Unfortunately, upper air observations were sparse or nonexistent during much of the period covered by the 20th century reanalysis used here, so that it is not possible to compare the outflow temperatures calculated from this reanalysis with observations. Instead, we compare the outflow temperatures of two different reanalyses that assimilated all available upper air observations during the period 1980–2001: the NCAR/NCEP reanalysis (Kalnay and co-authors, 1996) and the ERA-40 reanalysis (Uppala and co-authors, 2006). Figure 13a compares the time series of ERA-40-derived outflow temperature averaged over the Atlantic Main Development Region during August–October with that calculated from the NCAR/NCEP reanalysis over the same region and period. Beginning in the early 1990s, there is a large downward trend in the NCAR/NCEP-derived outflow temperature, resulting in a decline of almost 5 degrees over about 12 years. But there is no trend in the

ERA-40-derived outflow temperature during this period. Figure 13b compares the potential intensities over this region and period; while the ERA-40 series shows no trend, there is a significant upward trend in the NCAR/NCEP-derived potential intensity. Figure 13c compares a measure of the air-sea thermodynamic disequilibrium between the two products, showing that this contribution to the potential intensity is not responsible for the differing trend in potential intensity; in fact, the trend in ERA-40 is significantly larger.

Figure 14 compares the annual tropical cyclones numbers downscaled from the NCAR/NCEP and ERA-40 reanalyses to best-track data for the period 1980–2001. The trend of the NCEP-downscaled counts is very nearly equal to the observed trend, while the ERA-40-downscaled trend is much less; moreover, the NCEP-downscaled counts are highly correlated with the observed frequency of events ($r^2 = 0.65$), while the ERA-40-downscaled counts are uncorrelated with the best-track data. The evidence presented here points to the lack of trend in outflow temperature in the ERA-40 reanalysis as the principal culprit in the underprediction of the downscaled storm frequency trend. This leads to an underprediction of the trend in potential intensity (Figure 13b), which influences the downscaled storm counts.

4. Summary

We have applied a recently developed technique for downscaling tropical cyclone activity to the NOAA-CIRES 20th century reanalysis, a global reanalysis driven only by surface temperature, sea ice, and surface pressure observations during the period 1908–1958. Because this reanalysis is free from upper air and satellite observations, it does not suffer from the degree of bias caused by the changing number and type of such observations that are known to affect more complete reanalyses such as the NCAR/NCEP reanalysis of the period 1949 to the present.

The downscaling shows a significant decline in the frequency and power dissipation of events in the Southern Hemisphere over the period, but increasing frequency and power dissipation in the North Atlantic, eastern North Pacific, and North Indian oceans. Comparison with observed (best-track) data in the North Atlantic region (the only region with somewhat reliable data over this period) shows that upward trends in the downscaled frequency and power dissipation are smaller than those in the best-track data. Some of this may be owing to underestimation of the frequency of events early in the period (Chang and Guo, 2007, Vecchi and Knutson, 2008), but the best linear fit of the downscaled to the observed power dissipation shows that both the trend and the multi-year variability are underestimated by similar factors, suggesting that the underestimation of the variability and of the trend may have the same cause. The number of downscaled short-duration events increases significantly in the North Atlantic during

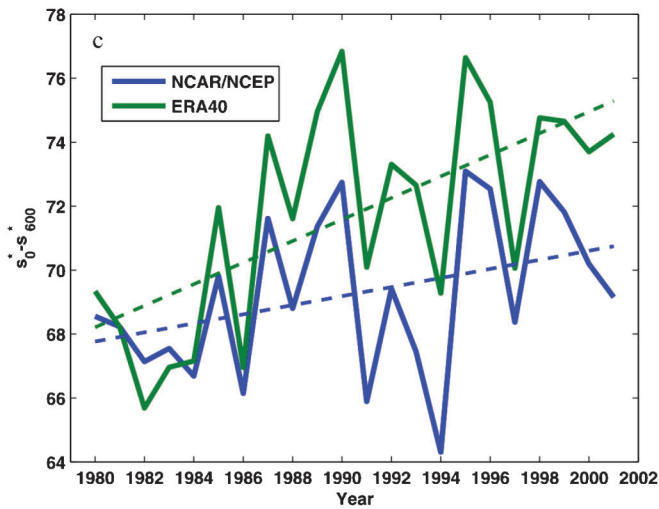
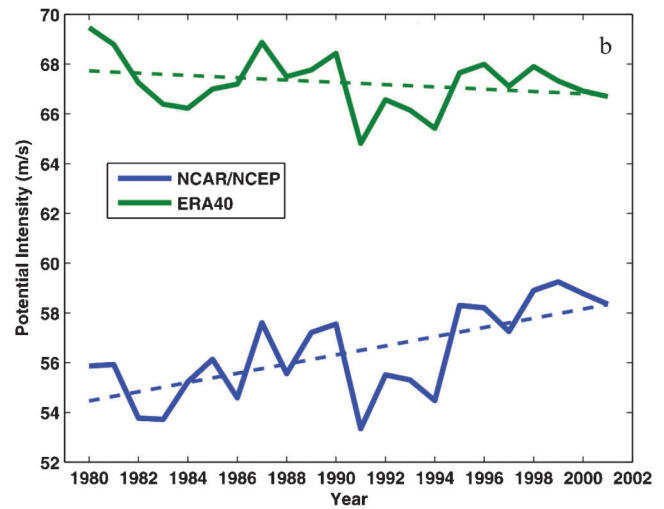
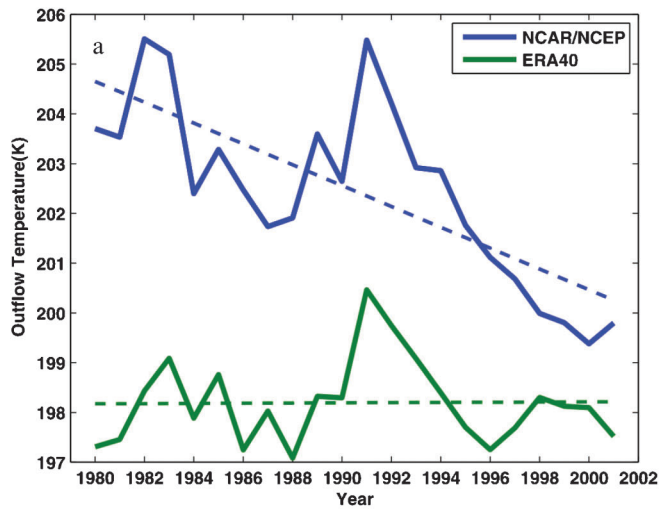


Figure 13: Comparison of ERA-40-derived (green) with NCAR/NCEP reanalysis-derived (blue) outflow temperatures (a), potential intensity (b), and air-sea thermodynamic disequilibrium (c) during the years 1980-2006. Values are averaged over the Atlantic genesis region, August-October. In (c), the metric is saturation entropy of the sea surface minus saturation entropy at 600 hPa.

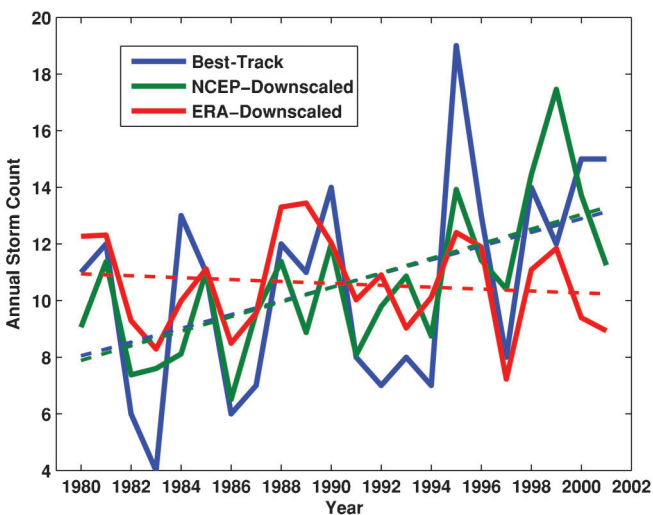


Figure 14: Comparison of Atlantic annual storm counts from best-track data (blue) to those from the NCAR/NCEP (green) and ERA-40 (red) reanalyses. Linear trends are superimposed.

the period, suggesting that the hypothesis of Landsea et al. (2009) that the observed increase in the number of short duration events is mostly or entirely owing to changing observations may not be correct.

Comparison of the downscaled event frequencies with a new genesis potential index shows good agreement on small regional scales, but poor agreement on global and larger regional scales (such as the whole of the western North Pacific tropical cyclone region). This suggests that the new index captures those climate influences that act on small regional scales, but is not as successful in capturing global signals.

In interpreting these results, it must be noted that the correct specification of sea surface temperatures does not necessarily produce the correct mean state of the atmosphere. In particular, we showed here that incorrect specification of radiative transfer through the model's atmosphere owing, for example, to the incorrect specification of greenhouse gases or clouds, will necessarily lead to

energy imbalance at the sea surface and thereby to an incorrect potential intensity. We also showed that variations in the outflow temperature, which is a function of both atmospheric temperature and sea surface temperature, have a strong influence on trends in downscaled tropical cyclone activity, and that one of the two standard reanalyses over the period 1980-2001 produces much smaller trends in outflow temperature than does the other. Given the high negative correlation between observed trends in sea surface temperature and temperature of the upper troposphere and lower stratosphere (Fu et al., 2006) and the failure of GCMS to capture this (Cordero and Forster, 2006), one must treat the quantitative prediction of the response of potential intensity to global warming with appropriate skepticism.

Acknowledgement: The work reported on here was supported by the National Science Foundation under grant 0850639.

References

- Bengtsson, L., M. Botzet, and M. Esch, 1996: Will greenhouse-induced warming over the next 50 years lead to higher frequency and greater intensity of hurricanes? *Tellus*, **48A**, 57-73, doi: [10.1034/j.1600-0870.1996.00004.x](https://doi.org/10.1034/j.1600-0870.1996.00004.x).
- Bengtsson, L., K. I. Hodges, M. Esch, N. Keenlyside, L. Kornbleuh, J.-J. Luo, and T. Yamagata, 2007: How may tropical cyclones change in a warmer climate? *Tellus*, **59**, 539-561, doi: [10.1111/j.1600-0870.2007.00251.x](https://doi.org/10.1111/j.1600-0870.2007.00251.x).
- Bister, M., and K. A. Emanuel, 1998: Dissipative heating and hurricane intensity. *Meteor. Atmos. Physics*, **50**, 233-240, doi: [10.1007/BF01030791](https://doi.org/10.1007/BF01030791).
- Bister, M., and K. A. Emanuel, 2002: Low frequency variability of tropical cyclone potential intensity, 1: Interannual to interdecadal variability. *J. Geophys. Res.*, **107**, doi: [10.1029/2001JD000776](https://doi.org/10.1029/2001JD000776).
- Chang, E. K. M., and Y. Guo, 2007: Is the number of North Atlantic tropical cyclones significantly underestimated prior to the availability of satellite observations? *Geophys. Res. Lett.*, **34**, doi: [10.1029/2007GL030169](https://doi.org/10.1029/2007GL030169).
- Compo, G. P., J. S. Whitaker, and P. D. Sardeshmukh, 2006: Feasibility of a 100 year reanalysis using only surface pressure data. *Bull. Amer. Meteor. Soc.*, **87**, 175-190, doi: [10.1175/BAMS-87-2-175](https://doi.org/10.1175/BAMS-87-2-175).
- Compo, G. P., J. S. Whitaker, and P. D. Sardeshmukh, 2008: The 20th century reanalysis project. *Third WCRP International Conference on Reanalysis*.
- Cordero, E. C., and P. M. Forster, 2006: Stratospheric variability and trends in models used for the IPCC AR4. *Atmos. Chem. Phys.*, **6**, 5369-5380.
- Emanuel, K., and D. Nolan, 2004: Tropical cyclone activity and the global climate system. *26th Conference on Hurricanes and Tropical Meteorology*, Miami, Amer. Meteor. Soc., 240-241.
- Emanuel, K., R. Sundarajan, and J. Williams, 2008: Hurricanes and global warming: Results from down-scaling IPCC AR4 simulations. *Bull. Amer. Meteor. Soc.*, **89**, 347-367, doi: [10.1175/BAMS-89-3-347](https://doi.org/10.1175/BAMS-89-3-347).
- Emanuel, K. A., 1986: An air-sea interaction theory for tropical cyclones. Part I. *J. Atmos. Sci.*, **42**, 1062-1071, doi: [10.1175/1520-0469\(1986\)043<0585:AASITF>2.0.CO;2](https://doi.org/10.1175/1520-0469(1986)043<0585:AASITF>2.0.CO;2).
- Emanuel, K. A., 2005: Increasing destructiveness of tropical cyclones over the past 30 years. *Nature*, **436**, 686-688, doi: [10.1038/nature03906](https://doi.org/10.1038/nature03906).
- Fairall, C. W., E. F. Bradley, J. E. Hare, A. A. Grachev, and J. B. Edson, 2003: Bulk Parameterization of Air-Sea Fluxes: Updates and Verification for the COARE Algorithm. *J. Climate*, **16**, 571-591, doi: [10.1175/1520-0442\(2003\)016<0571:BPOASF>2.0.CO;2](https://doi.org/10.1175/1520-0442(2003)016<0571:BPOASF>2.0.CO;2).
- Fu, Q., C. M. Johanson, J. M. Wallace, and T. Reichler, 2006: Enhanced mid-latitude tropospheric warming in satellite measurements. *Science*, **312**, 1179, doi: [10.1126/science.1125566](https://doi.org/10.1126/science.1125566).
- Gray, W. M., 1979: Hurricanes: Their formation, structure, and likely role in the tropical circulation. *Meteorology over the tropical oceans*, B. Shaw, Ed., Roy. Meteor. Soc., 155-218.
- Kalnay, E., and co-authors, 1996: The NCEP/NCAR 40-year reanalysis project. *Bull. Amer. Meteor. Soc.*, **77**, 437-471, doi: [10.1175/1520-0477\(1996\)077<0437:TNYRP>2.0.CO;2](https://doi.org/10.1175/1520-0477(1996)077<0437:TNYRP>2.0.CO;2).
- Knutson, T. R., J. J. Sirutis, S. T. Garner, I. M. Held, and R. E. Tuleya, 2007: Simulation of the recent multi-decadal increase of Atlantic hurricane activity using an 18-km grid regional model. *Bull. Amer. Meteor. Soc.*, **88**, 1549-1565, doi: [10.1175/BAMS-88-10-1549](https://doi.org/10.1175/BAMS-88-10-1549).
- Landsea, C. W., and co-authors, 2004: The Atlantic hurricane database re-analysis project: Documentation for the 1851-1910 alterations and additions to the HURDAT database. *Hurricanes and Typhoons: Past, Present and Future*, J. Murnane, and K.-B. Liu, Eds., Columbia Univ. Press, 177-221.
- Landsea, C. W., G. A. Vecchi, L. Bengtsson, and T. R. Knutson, 2009: Impact of Duration Thresholds on Atlantic Tropical Cyclone Counts. *J. Climate*, **22**, in press, doi: [10.1175/2009JCLI3034.1](https://doi.org/10.1175/2009JCLI3034.1).
- Neumann, C. J., B. R. Jarvinen, C. J. McAdie, and G. R. Hammer, 1999: Tropical cyclones of the North Atlantic Ocean, 1871-1998. National Climatic Data Center/Tropical Prediction Center/National Hurricane Center 6-2, 206 pp.
- Oouchi, K., J. Yoshimura, H. Yoshimura, R. Mizuta, S. Kusunoki, and A. Noda, 2006: Tropical cyclone climatology in a global-warming climate as simulated in a 20 km-mesh global atmospheric model: Frequency and wind intensity analyses. *J. Meteor. Soc. Japan*, **84**, 259-276, doi: [10.2151/jmsj.84.259](https://doi.org/10.2151/jmsj.84.259).
- Pielke, R. A. J., and C. W. Landsea, 1998: Normalized hurricane damages in the United States, 1925-1995. *Wea. and Forecast.*, **13**, 621-631, doi: [10.1175/1520-0434\(1998\)013<0621:NHDITU>2.0.CO;2](https://doi.org/10.1175/1520-0434(1998)013<0621:NHDITU>2.0.CO;2).

- Rennó, N. O., K. A. Emanuel, and P. H. Stone, 1994: Radiative-convective model with an explicit hydrological cycle, Part I: Formulation and sensitivity to model parameters. *J. Geophys. Res.*, **99**, 14429-14441, doi: [10.1029/94JD00020](https://doi.org/10.1029/94JD00020).
- Rotunno, R., Y. Chen, W. Wang, C. Davis, J. Dudhia, and C. L. Holland, 2009: Large-eddy simulation of an idealized tropical cyclone. *Bull. Amer. Meteor. Soc.*, **90**, 1783-1788, doi: [10.1175/2009BAMS2884.1](https://doi.org/10.1175/2009BAMS2884.1).
- Santer, B. D., and co-authors, 1999: Uncertainties in observationally based estimates of temperature change in the free atmosphere. *J. Geophys. Res.*, **104**, 6305-6333, doi: [10.1029/1998JD200096](https://doi.org/10.1029/1998JD200096).
- Sriver, R., and M. Huber, 2006: Low frequency variability in globally integrated tropical cyclone power dissipation. *Geophys. Res. Lett.*, **33**, doi: [10.1029/2006GL026167](https://doi.org/10.1029/2006GL026167).
- Sugi, M., A. Noda, and N. Sato, 2002: Influence of the global warming on tropical cyclone climatology: An experiment with the JMA global climate model. *J. Meteor. Soc. Japan*, **80**, 249-272, doi: [10.2151/jmsj.80.249](https://doi.org/10.2151/jmsj.80.249).
- Uppala, S. M., and co-authors, 2006: The ERA-40 Re-analysis. *Quart. J. Roy. Meteor. Soc.*, **131**, 2961-3012, doi: [10.1256/qj.04.176](https://doi.org/10.1256/qj.04.176).
- Vecchi, G. A., and T. R. Knutson, 2008: On estimates of historical North Atlantic tropical cyclone activity. *J. Climate*, **21**, 3580-3600, doi: [10.1175/2008JCLI2178.1](https://doi.org/10.1175/2008JCLI2178.1).
- Yoshimura, J., S. Masato, and A. Noda, 2006: Influence of greenhouse warming on tropical cyclone frequency. *J. Meteor. Soc. Japan*, **84**, 405-428, doi: [10.2151/jmsj.84.405](https://doi.org/10.2151/jmsj.84.405).
- Zhao, M., I. M. Held, S.-J. Lin, and G. A. Vecchi, 2009: Simulations of global hurricane climatology, interannual variability, and response to global warming using a 50km resolution GCM. *J. Climate*, **22**, 6653-6678, doi: [10.1175/2009JCLI3049.1](https://doi.org/10.1175/2009JCLI3049.1).